

Composite Fading in Downlink Cooperative Heterogeneous Networks



By

Atta ur Rahman

2012-NUST-MS-EE-60854

Supervisor

Dr. Syed Ali Hassan

Department of Electrical Engineering

A thesis submitted in partial fulfillment of the requirements for the degree
of Masters in Electrical Engineering (MS EE-TCN)

In

School of Electrical Engineering and Computer Science,
National University of Sciences and Technology (NUST),

Islamabad, Pakistan.

(June 2015)

Approval

It is certified that the contents and form of the thesis entitled “**Composite Fading in Downlink Cooperative Heterogeneous Networks**” submitted by **Atta ur Rahman** have been found satisfactory for the requirement of the degree.

Advisor: **Dr. Syed Ali Hassan**

Signature: _____

Date: _____

Committee Member 1: **Dr. Khawar Khrshid**

Signature: _____

Date: _____

Committee Member 2: **Dr. Adnan Khalid Kiani**

Signature: _____

Date: _____

Committee Member 3: **Dr. Hassaan Khaliq**

Signature: _____

Date: _____

Abstract

The need for small-sized and low-powered home base stations such as femtocells has increased with an escalated data demand. Since the downlink traffic is larger in magnitude than the uplink, use of femtocells provides a good solution. Femtocells not only increase the throughput but also the overall capacity of the system while operating in the same licensed spectrum. Because of their operation in the same spectrum, interference becomes a major problem. In this work, we study the downlink performance of a heterogeneous network. We proposed Reverse frequency allocation (RFA) scheme by dividing the cell service area into multiple regions and assign frequencies to various cell entities in such a way that the major interference is avoided. RFA scheme not only improves the spectral efficiency but also eliminates the strong interference due to macro base station on femto users. We focused on shadowing and multipath fading, which are two fundamental channel characteristics that impact the performance of a wireless communication system. We have analyzed the performance of device to device (D2D) cooperative heterogeneous networks where idle femtocell users can be engaged to provide better coverage to a macrocell user using amplify-and-forward cooperative strategy. We consider multipath fading and lognormal shadowing along with path loss and model their effects on the performance of the network. Closed-

form expressions for the signal-to-noise ratio (SNR) and outage probabilities are derived and it has been shown that the downlink performance of the macrocell user can be enhanced by employing femto user cooperation.

Dedication

In the loving memory of my father without whom I am nothing.

Certificate of Originality

I hereby declare that this submission is my own work and to the best of my knowledge it contains no materials previously published or written by another person, nor material which to a substantial extent has been accepted for the award of any degree or diploma at National University of Sciences & Technology (NUST) School of Electrical Engineering & Computer Science (SEECS) or at any other educational institute, except where due acknowledgement has been made in the thesis. Any contribution made to the research by others, with whom I have worked at NUST SEECS or elsewhere, is explicitly acknowledged in the thesis.

I also declare that the intellectual content of this thesis is the product of my own work, except for the assistance from others in the project's design and conception or in style, presentation and linguistics which has been acknowledged.

Author Name: **Atta ur Rahman**

Signature: _____

Acknowledgment

I am very thankful to Allah who gave me strength, support and special blessing on me without all this; it cannot be possible for me to complete my research.

I would like to express my deepest gratitude to my advisor, Dr. Syed Ali Hassan, for his excellent guidance, patience and constant support. His invaluable help of constructive comments and suggestions throughout the thesis work have contributed to the success of this research.

Many thanks to my committee members for their support and help. My special thanks to all my friends who were always there for me specially Mud-dasar, Aamra, Rehan, Arslan, and many others.

Last but not least, my gratitude to my parents for their endless love, prayers and encouragement.

Atta ur Rahman

Table of Contents

1	Introduction	1
1.1	Problem Statement	4
1.2	Thesis Contribution	4
1.3	Thesis Organization	5
1.3.1	Chapter 2	5
1.3.2	Chapter 3	5
1.3.3	Chapter 4	5
1.3.4	Chapter 5	6
1.3.5	Chapter 6	6
2	Literature Review and Background	7
2.1	Frequency Allocation Schemes	7
2.2	Wireless Cooperative Communication in HetNets	9
3	Reverse Frequency Allocation Scheme	11
3.1	Reverse Frequency Allocation	11
3.2	Interference Modeling and Region Selection	14
3.2.1	Optimal Partitioning of Regions	15

<i>TABLE OF CONTENTS</i>	viii
4 Composite fading in HetNets	18
4.1 System Model	18
4.2 System Outage Analysis	21
5 Results and Analysis	26
5.1 Reverse Frequency Allocation	27
5.2 Cooperative Networks with individual channel impairments . .	31
6 Conclusions and Future Work	37
6.1 Conclusions	37
6.2 Future Work	39

List of Figures

3.1	Reverse frequency allocation of 4 regions.	12
3.2	Worst-case scenario in 4-region RFA. The direction of arrows shows the interference direction.	16
4.1	Simplistic model of cooperative communication through relays	20
5.1	Effects of β on coverage for various number of participating relays.	27
5.2	Effects of β on coverage for various number of participating relays.	28
5.3	Effects of β on coverage for various number of participating relays.	30
5.4	Effects of β on coverage for various number of participating relays.	31
5.5	The CDF of (a) χ_{ij} , product of exponential & lognormal RV., (b) SNR from relayed path., (c) Total SNR of the system. . .	32
5.6	Effects of β on coverage for various number of participating relays.	34
5.7	Effects of threshold SNR on system's coverage.	35

5.8 Variation in system's coverage for values of σ in large (left)
and small (right) cell environments 36

Chapter 1

Introduction

Femtocell is a low complexity, low-powered, and small-sized base station (BS) that enables communication with an improved quality of service. These base stations are placed inside user's premises but operate in licensed spectrum. As the demand for cellular services can originate from indoor environment significantly, hence it is desirable to provide good coverage to the indoor users. According to [1], by the start of 2011, approximately 2.3 million femtocells were globally deployed, and it is expected to reach approximately 50 million by 2014. Another study claims that 30% business and 45% home users are unsatisfied with their indoor coverage [2]. Because of an increase in the data demand, femtocells are gaining attention from mobile operators. The main purpose of the femtocells is to provide better indoor coverage while offloading traffic from the main macro base station (MBS), which indeed is an expensive radio resource.

While deploying a homogenous femto-cellular network, interference is one of the main problems since femtocells use the same spectrum as being utilized by overlaid macro-cellular network. These interferences are generally cate-

gorized as co-tier and cross-tier interference [3]. Co-tier interference occurs when transmission of one femtocell (aggressor) obstruct the on-going transmission of another femtocell and its user (victim). Cross-tier interference, on the other hand, adds extra degree of complexity. In cross-tier, the transmission between MBS (aggressor) and macro user equipment (MUE) interferes with the ongoing transmission between the femtocell access point (FAP) and femtocell user equipment FUE (victim) and vice versa. Cross-tier interference in femto-cellular environment is different from traditional interference. In closed-access mode of the femto-cellular network, the MUE would not be able to access femtocell's services. This would lead to a strong interference from MUE to FAP in the uplink operation and from FAP to MUE in the downlink operation.

For interference cancellation or avoidance, many schemes have been proposed that focus on different frequency allocation schemes. Selection of those allocation schemes is dependent upon femtocells density. One of the strategies is *static frequency-reuse* scheme in which the bands for macrocell and femtocell are dedicated separately [4]. In *shared frequency band* scheme, the total spectrum can be utilized by both macro and femtocell, while in sub-frequency band scheme; the whole spectrum is allotted to macrocell while a portion of the whole band is fixed for the femtocells. In this paper, we use the shared frequency allocation scheme and propose a variant of this scheme known as Reverse frequency allocation (RFA). In RFA, we divide the complete cell in non-overlapping regions and frequency band is distributed in such a way that spectral efficiency can be improved. Due to partitioning of cell, the number of interferers, i.e., users operating on the same frequency

can also be reduced.

Talking about the QoS parameters like increased coverage, high data rates, and improved spectral efficiency are becoming critical parameters in the next generation cellular networks. Device to device (D2D)-based heterogeneous networks (HetNets) have gained enormous attention because of their capability of achieving these goals. In a general HetNet, small base stations (BS), also known as femtocells, are deployed within a macrocell that provide coverage to their intended users through different access modes. D2D communication is also considered as a key component of Long Term Evolution-Advanced (LTE-A) in which devices directly communicate with each other resulting in improved local services [5]. D2D communication occurs when devices are in close proximity with each other, reducing not only the communication cost by eliminating redundant cellular direct transmission but also improving the spectral efficiency.

Cooperative communication in D2D-based HetNets also helps in achieving the desired goals, e.g., femtocell user equipment (FUE) in an idle state can utilize capabilities to enhance the coverage of a macrocell user equipment (MUE), which is distant to its serving BS. The BS broadcasts the signal to its intended MUE, however the overheard signal by the idle FUEs can be relayed to the MUE and can be used to enhance its decoding capability. Carrying out BS controlled D2D communication in a HetNet offers many challenges, which include interference, path loss, multipath fading, and shadowing. While modeling large-scale networks, shadowing should be taken into consideration as it significantly degrades the quality of the signal. Until now, most of the work in D2D communication has been done considering

deterministic models, e.g., path loss, or only fading is considered as the only channel impairment as in [6].

1.1 Problem Statement

“Channel modeling of a heterogeneous network is done in order to improve system’s throughput by enabling Cooperation between users to improve system’s throughput, while incorporating fading, path loss, and shadowing effected channels as independent channel impairment parameters. In all literature, these impairment parameters are considered as single channel impairment parameter.

”

1.2 Thesis Contribution

The objective of this paper is to analyze how cooperative communication helps a macro user, which is weakly connected to its BS in the presence of composite fading. For that we derive the analytical expression for the signal-to-noise ratio (SNR) at the destination node in presence of FUEs cooperation. We then further derive the outage probability of the destination node assuming a lognormal distribution of the received SNR. We have shown that an increase in the severity of shadowing badly impacts the performance of system under consideration.

1.3 Thesis Organization

The rest of the thesis is organized as follows.

1.3.1 Chapter 2

Chapter 2 describes the background and literature review of the thesis. In this chapter, different types of frequency allocation schemes are explained e.g., soft frequency Reuse, fractional frequency reuse, and different types of other allocation schemes. The use of cooperative communication in wireless network is also discussed. Effects of different channel impairments on quality of service is also discussed in this chapter.

1.3.2 Chapter 3

In chapter 3, system architecture of Reverse frequency allocation scheme is discussed. Different modes of RFA with respect to different cell regions is discussed in detail. Optimal partitioning of cell region is also taken under consideration. Interferences has been modeled by taking under consideration different scenarios which includes multiple cell regions, different cell radii, etc. Trade off between spectral efficiency and total number of served users is also discussed in the later part of this chapter.

1.3.3 Chapter 4

In chapter 4, detailed analysis of different channel impairments like shadowing, multipath fading, and path loss has been done. We modeled the resulting SNR, which include the above mentioned impairments, through

proper distribution. Closed form mathematical equations of the resulting mean and variance are derived. It is proved that the resulting PDF can be modeled through the lognormal distribution. All the analysis has been done considering the HetNet environment implying cooperative communication.

1.3.4 Chapter 5

In Chapter 5, we compare our analytical results with simulations. We show the optimal performance of the RFA scheme in different partitions, number of relays, path loss exponents. Also the effects of channel impairments is observed in this section. We proved that the shadowing must be considered individually in order to obtain optimal results. We also proved that in a cooperative HetNet, the resulting SNR can be modeled properly through the lognormal distribution. Analysis of different shadowing, path loss, multipath fading, and threshold SNR for this scenario is also discussed in detail.

1.3.5 Chapter 6

The thesis conclusion and future work is discussed in this chapter.

Chapter 2

Literature Review and Background

2.1 Frequency Allocation Schemes

A complete introduction about femtocells including all types of interference scenarios is presented in [7], along with other papers such as [8]-[11]. Regarding interference avoidance in femtocells, many researchers proposed different frequency planning techniques. Initially, it was proposed to assign different orthogonal frequencies to the base stations of different cells [12]. Authors in [13] proposed another elegant scheme of *fractional frequency reuse* (FFR). In FFR, whole of the spectrum is divided into multiple frequency bands. These bands are distributed among cluster such that the users that are present in the middle of the cell are allocated with a separate band from the users that are present at the edge. Although this schemes allocates different frequency bands to the edge-users and the users present in the center of the cell, but still it is spectrally inefficient as the available resources may not be used

efficiently.

The authors of [14] proposed *soft fractional frequency reuse* scheme. This schemes also partitions the whole frequency spectrum but allows the center-cell users to use more than one frequency bands. It is spectrally more efficient as compared to previous scheme because femto users can also utilize the same band that is assigned to the macro users. The whole band is utilized within a single cell, which also makes it spectrally more efficient. The drawback of this scheme is that part of band is still statically dedicated for femto users and also like the previous schemes, this scheme does not take account of user's traffic distribution.

The authors of [15] proposed a simple algorithm which provides more preference to the MUE's by controlling the power of the FAP. The fundamental assumption is that, MBS provides the information of MUE's to all the FAPs. Once the MUE's is under significant interference, the nearby FAP will reduce its transmit power. This approach leads to the performance degradation of FUE's. Another approach which is used to avoid the interference in OFDMA based femtocells is discussed in [11]. In this approach, each FAP initially sense the surrounding radio environment for specific sub-channel. Each user equipment requires a certain number of sub-channels depending upon the QoS criteria. If a particular sub-channel is free, FAP then allocate the sub-channel to that user, subject to low level of interference.

The authors of [16] proposed a *dynamic frequency reuse* scheme that considers the overall traffic load. The spectrum allocation for both the macro and femto regions changes dynamically depending upon the traffic load pattern. However, the drawback of this scheme is that it is highly dependent

upon current information about geographical locations of the users. Technique that is analyzed in [17] is *reverse frequency allocation* scheme (RFA). Reverse Frequency allocation scheme divides the complete region into two non-overlapping regions named as inner region and outer region. It is spectrally most efficient among all the schemes because it not only utilizes whole frequency band among single cell but also the frequencies used for the uplink and the downlink transmissions of MBS to MUE are being utilized as the downlink and uplink frequencies of FAP to FUE, respectively. In this work, we extend this approach by allowing multiple regions in a cell. Specifically, we demonstrate a 4-region RFA scheme and compare its performance with the 2-region RFA as discussed in [17].

2.2 Wireless Cooperative Communication in HetNets

There are many challenges that are faced during a HetNet deployment, which includes interference, path loss, multipath fading, and shadowing to name a few. While modeling large-scale networks, shadowing is a major factor, which should be taken into consideration as it can significantly degrades the quality of the signal. The shadowing models the random variations in the received power observed over such large distances, which are equivalent to the widths of large reflectors like buildings. On the other hand multipath fading is generally modeled through Rayleigh, Nakagami or Rice distributions[18,19]. However, in many cases both multipath fading and shadowing occurs at the same time and leads to a composite distribution. The composite Rayleigh-

lognormal distribution[18] is widely used to model the composite fading that includes multi-path fading and shadowing.

In [20], authors derived the mathematical expressions of bit error and outage probabilities for opportunistic and conventional relay environment. They considered channels to be Rician faded. Authors in [21] has modeled the bit error rate in Rician faded channels. They considered cooperation between the nodes. Relays follow amplify-and-forward mechanism. Like [20], they also considered path loss, shadowing and channel fading a single parameter. Rician fading consider the presence of line of sight LOS link between the transmission antenna and the receiver which however is not true in every case. Cooperative models are often more required/advantageous where there is no LOS link.

In [22], authors modeled presented bit error rate analysis of Rayleigh faded channels in cooperative networks. Rayleigh fading is generally used when there is no LOS link between the transmitter and the receiver node. They also considered the combined effect of path loss, channel fading and shadowing. These parameters have individual effects on the system and need to be modeled separately. Drawback is complex mathematical derivations but the resultant expressions yield more practical results.

Chapter 3

Reverse Frequency Allocation Scheme

In this chapter, the system model that has been adapted for RFA scheme, and their parameters are described.

3.1 Reverse Frequency Allocation

We consider a reverse frequency allocation (RFA) scheme for a single cell in which the entire region of a macrocell is divided into k disjoint regions. Furthermore, the allocated frequency spectrum, F , is divided among k orthogonal sub-bands, such that $F = \bigcup_{i=1}^k F_i$, where $\bigcap_{i=1}^k F_i = \phi$; ϕ denotes a empty set.

For every i^{th} region, we assume frequency division duplexing (FDD), i.e., each sub-band is further divided into its uplink and downlink frequency bands, such that

F ₁		F ₂		F ₃		F ₄	
R ₁ Macrocell UL	R ₁ Macrocell DL	R ₂ Macrocell UL	R ₂ Macrocell DL	R ₃ Macrocell UL	R ₃ Macrocell DL	R ₄ Macrocell UL	R ₄ Macrocell DL
F_{1A}	F_{1B}	F_{2A}	F_{2B}	F_{3A}	F_{3B}	F_{4A}	F_{4B}
R ₃ Femtocell DL	R ₃ Femtocell UL	R ₄ Femtocell DL	R ₄ Femtocell UL	R ₁ Femtocell DL	R ₁ Femtocell UL	R ₂ Femtocell DL	R ₂ Femtocell UL

Figure 3.1: Reverse frequency allocation of 4 regions.

$$F_i = \left[F_{iA} + F_{iB} ; \right.$$

$$\left. i = \{1, 2, \dots, k\} . \right.$$

For a fair usage of frequencies in the RFA scheme, we assume $k=2^M$, where $M \in Z^+ = \{1, 2, \dots\}$.

In the following, we consider $k=4$ and provide a complete spectral decomposition of the network for a 4-region RFA scheme. As mentioned earlier, the basic aim of the RFA scheme is to divide a cellular region in such a way that least amount of interference scenarios are produced; thereby decreasing the overall outage of the system. For that as shown in Fig. 3.1, the available region is divided into four non overlapping regions, i.e., R_1 , R_2 , R_3 , and R_4 , respectively. The available spectrum F for the single cell is also divided into 4 bands namely F_1 , F_2 , F_3 , and F_4 and each region is assigned a frequency band. Each band contains the uplink and downlink frequency carriers. Frequency carriers F_{1A} and F_{1B} are used by MUEs in R_1 , F_{2A} & F_{2B} for MUEs in R_2 for uplink and downlink operations, and so on. It can be observed that

the MBS have relatively high transmit power as compared to FAPs, hence the femto users receive large amount of interference from MBS on the same frequency channel. Thus it is desired to allocate the frequencies in such a way that a femto user receives no interference from the downlink of MBS. Hence if F_{1A} is used for downlink FUEs in R_3 , it is desired to reuse this frequency for one of the uplinks of MUEs in R_1 , and interference is minimal if these two interfering regions are as far as possible. Hence we make two sets of interfering regions; R_1 & R_3 , and R_2 & R_4 . Hence this implies that R_1 -FUE in downlink uses the same frequency as the uplink MUE in R_3 .

Since our focus for this study is the downlink receiver (mobile users either MUEs or FUEs), hence the interference arrives from R_3 -FAP to R_1 -MUE. As FAPs are low powered and large path loss exists between these nodes this interference is not significant. On the other hand, the R_1 -MUE in uplink uses the same frequency as that of the downlink FUE in R_3 . In this case, the downlink FUE receives interference from MUE uplink, which is again low-powered and feeble because of the path loss between R_1 and R_3 . Hence minimal interference is observed using this scheme for both downlink users, i.e., R_1 -MUE and R_3 -FUE. Same procedure is done for R_2 and R_4 . In summary, the frequencies are allocated to the femtocells in such a way that the femtocells that are contained in R_1 will use F_{3A} and F_{3B} frequency carriers for their downlink and uplink operations, respectively. Similarly, R_2 femtocells will use F_{4A} and F_{4B} frequency carriers for downlink and uplink operations, respectively. In the same way, R_3 and R_4 femtocells will utilize F_{1A} , F_{1B} and F_{2A} , F_{2B} frequency carriers for their downlink and uplink operations, respectively.

3.2 Interference Modeling and Region Selection

As described earlier, the interference in this particular case of 4-region RFA arrives from only one interfering region. For example, communication going on in R_1 will be interfering the communication of R_3 as they are operating on the same partitioned frequency, i.e., F_1 . Interference, on the other hand, will be significantly reduced because in the 4-region case the area under each region is minimized. As the area is reduced the number of interferers will also be reduced on the average.

Although the RFA scheme offers more vulnerability to interference, however, interference either co-tier and/or cross-tier both will have their impact on the downlink users performance metrics. These performance metrics can be throughput and coverage etc. In heterogeneous networks a designer must, due to different channel conditions, prioritize these performance metrics. For example, in an environment of high user density the system must optimize its spectral efficiency so that greater number of users can be adjusted. While on the other hand a system that ensures high data rate must optimize to certify high SINR. In each case the other performance metric can be sub-optimized.

We now model the various types of interferences present in our system. As described, the FUEs encounter interference not only from uplink MUEs in the distant region but also from the neighboring FAPs in the same region that are operating at the same frequency. As this work studies the outage aspects of the network, which means that the SINR is the performance metric that will be used in this type of system. The SINR at a receiver j can be

calculated as

$$SINR(dB) = \frac{P_{des}}{d_{des}^\beta} \mu_{mj} - \sum_{i \in \mathbb{I}} \frac{P_i}{d_{ij}^\beta} \mu_{ij} \quad (3.1)$$

where P_{des} is the power received from the intended transmitter m , while P_i is the interfering power from the i th transmitter, which can be co-tier or cross-tier interferer. The set \mathbb{I} denotes the set of all interferers. The path loss exponent is represented as β , while the distances of the receiver from the interferers and desired transmitter are represented as d_{ij} and d_{des} , respectively. The flat fading channel gain from the desired and interfering transmitter to the j th receiver is denoted by μ_{mj} and μ_{ij} , respectively, where μ_{mj} , $\mu_{ij} \in \mu$ and the set μ consists of independently and identically distributed (i.i.d) random variables, which are drawn from an exponential distribution with the parameter $\sigma_\mu^2 = 1$. Hence we are interested in finding the $\mathbb{P}\{SINR \leq P_{th}\}$ and average this outage probability for all users of the system.

3.2.1 Optimal Partitioning of Regions

The multiple regions in the RFA must be partitioned in such a way that the impact of the interference should be minimized. For example, in Fig. 3.2, 4-region RFA is implemented in a cell with radius r , which is further divided into four non-overlapping regions. To find the optimal distance for each region, we consider a worst-case scenario, i.e., we want to calculate the optimal region lengths, when the interference in the system is maximum. As it is already been shown that the in a 4-region RFA, R_1 and R_2 are the interfering regions with R_3 and R_4 , respectively. The femto users (FUEs) are placed at the region boundaries while their interfering macro users (MUEs)

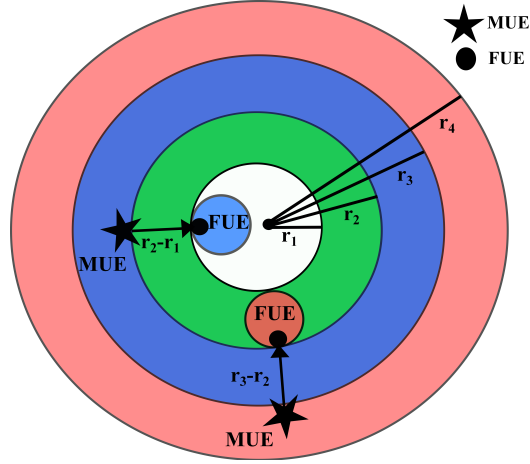


Figure 3.2: Worst-case scenario in 4-region RFA. The direction of arrows shows the interference direction.

are placed at their nearest interfering region's boundary. This is the worst-case scenario because the interference from each MUE to its respective FUE is maximum in this situation.

As the co-tier interference is one of the major contributing factors towards the total interference in this RFA scheme and will have a significant impact in R_1 . This is due to the fact that the density of the femtocells with respect to this area is highest in this region. So for a certain fixed threshold, P_{th} , through extensive simulations, it is observed that r_1 should be at least $0.6r$ so that the SINR of this particular region should be above an acceptable value. As in the worst-case, SINR should be at least equal to the P_{th} to get success, therefore, our optimization problem becomes the following;

$$\text{maximize } \{SINR\}$$

s.t

$$r_1 = 0.6r, \quad r_1 \leq r_2 \leq r_3 \leq r_4 \text{ and } r_4 = r, \text{ where } r_1, r_2, r_3 \text{ and } r_4 \text{ are the radius}$$

of R_1, R_2, R_3 and R_4 regions, respectively. To explain this approach, let us again consider the example of 4-region RFA. From Fig. 3.2,

$$SINR_{opt} = \frac{(r_2 - r_1)^2}{\delta_{FUE}} = P_{th}, \quad (3.2)$$

$$SINR_{opt} = \frac{(r_3 - r_2)^2}{\delta_{FUE}} = P_{th}, \quad (3.3)$$

where δ_{FUE} is the maximum distance of FUE from its intended FAP. From (3.2) and (3.3),

$$r_2 = \frac{(r_1 + r_3)}{2}. \quad (3.4)$$

As, $r_3 \leq r_4$ then $r_2 \leq 0.8r$. Now r_3 , due to fairness, is taken equal between r_2 and r_4 . So, $r_3 \leq 0.9r$.

This optimal analysis was tested in cells with different radii and is discussed in the results section.

Chapter 4

Composite fading in HetNets

As discussed in the previous sections, Cooperative Communication is a mode of communication in wireless systems in which nodes co-operate with each other to achieve common objectives. Cooperation can also be viewed as a means for mobile users to simply forward or relay each other's data to improve channel quality via diversity. We focused on deriving the outage probabilities of the overall system.

4.1 System Model

Consider an example of a heterogeneous two-tier network having both network and device centric entities participating, as depicted in Fig. 1. The base transceiver station (BTS) transmits the message signal with a certain transmit power to its MUE. In femtocell coverage regions, the femtocell access points (FAPs) are in transmission mode as well. We assume that all the FUEs located in the femtocell region are not in busy state, i.e., not having any data from FAP to send or receive. These users can establish D2D com-

munication by acting as relays and enhance the SNR of the macrocell user via cooperation. The destination will decide on the basis of its signal-to-interference plus noise ratio (SINR) whether to employ cooperation or not. The macrocell user, after realizing that the SINR is below a certain threshold will broadcast a message. These idle femtocell users, on reception of that message will broadcast their messages mentioning the SINR values that they are receiving from both FAP and the BTS. The end user can select the relays having the highest SINR values from the BTS and those idle femtocell users start relaying the signal towards destination through amplify-and-forward (AF) mechanism [23].

Empirical analysis has proved that shadowing can be modeled by a lognormal random variable (RV) [24] and the mean envelope power Ω_p corresponds following probability density function (PDF)

$$P_{\Omega_p}(x) = \frac{1}{x\sigma_{\Omega}\zeta\sqrt{2\pi}} \exp\left\{-\frac{(10\log_{10}\{x\} - \mu_{\Omega_p}(\text{dbm}))^2}{2\sigma_{\Omega}^2}\right\}, \quad (4.1)$$

where $\zeta = \frac{\ln(10)}{10}$, μ_{Ω_p} is the mean and σ_{Ω} is the shadow standard deviation. We consider a binary phase-shift keying (BPSK) modulation technique and assume that the channel is slow, flat faded and Rayleigh distributed where shadowing is also present. The power received at the destination because of BTS transmission is given as

$$P_r = \frac{P_t}{d_{ij}^{\beta}} h_{ij} S_{ij}, \quad (4.2)$$

where P_t is the power transmitted from the BTS and i and j are the source and destination nodes, respectively. S_{ij} is the large-scale fading channel gain, $S_{ij} \in S$, where S represents a lognormal RV, with mean μ and standard deviation σ . The flat fading channel gain is represented as $h_{ij} \in h$, where h

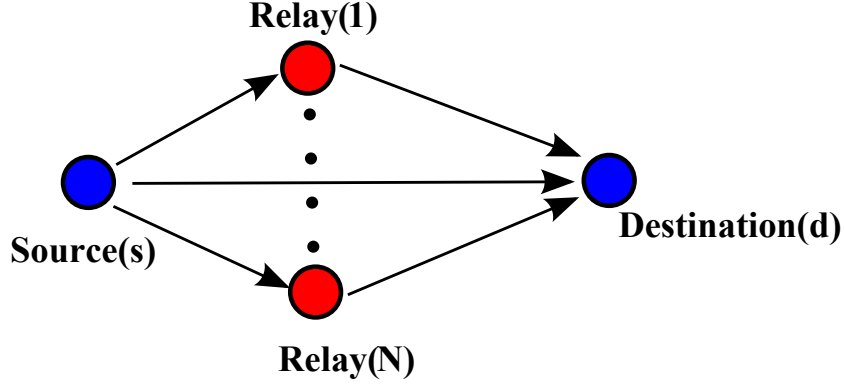


Figure 4.1: Simplistic model of cooperative communication through relays

represents a unit mean exponential RV, which is the squared envelope of the signal experiencing Rayleigh fading, the d_{ij} is the distance from the BTS to the destination and β is the path loss exponent.

A simplistic diagram of the system is depicted in Fig. 4.1. We begin our analysis by considering that the end user is receiving a BPSK modulated signal from the BTS. This signal is also being relayed to the destination user from different relays that are selected by the procedure mentioned earlier. The received signals at destination d from source s can be expressed as

$$Y_{sd} = h_{sd}\sqrt{S_{sd}}\sqrt{E_b}X_s + n_1, \quad (4.3)$$

where E_b is the bit energy sent by the source, X_s is the BPSK modulated signal and $n_1 \sim \mathcal{N}(0, \sigma_N^2)$ represents the Gaussian noise at the destination receiver. Similarly, the signal from source s to relay i can be written as

$$Y_{si} = h_{si}\sqrt{S_{si}}\sqrt{E_b}X_s + n_2. \quad (4.4)$$

We assume that each relay i on receiving the BTS signal forwards it to the destined end user d through AF principle, which can be expressed as

$$Y_{id} = \alpha_i(h_{si}\sqrt{S_{si}}\sqrt{E_b}X_s + n_2)h_{id} + n_3, \quad (4.5)$$

where amplification factor α_i of the relay i is expressed as

$$\alpha_i = \sqrt{\frac{E_i}{E_b |h_{si}|^2 S_{si} + \sigma_N^2}}. \quad (4.6)$$

All the received signals are combined at destination using maximal-ratio-combining (MRC) and the resultant signal Y_s becomes

$$Y_s = \frac{|h_{sd}|^2 S_{sd} E_b X_s}{\sigma_N^2} + \sum_{i=1}^N \frac{\alpha_i^2 |h_{si}|^2 |h_{id}|^2 S_{si} S_{id} E_b X_s}{\sigma_N^2 (\alpha_i^2 |h_{id}|^2 S_{id} + 1)}, \quad (4.7)$$

and the resultant noise signal Y_n can be expressed as

$$Y_n = \frac{h_{sd}^* \sqrt{S_{sd}} \sqrt{E_b} n_1}{\sigma_N^2} + \sum_{i=1}^N \left\{ \frac{\alpha_i^2 |h_{id}|^2 h_{si}^* S_{id} \sqrt{S_{si}} \sqrt{E_b} n_2}{\sigma_N^2 (\alpha_i^2 |h_{id}|^2 S_{id} + 1)} + \frac{\alpha_i^* h_{id}^* h_{si}^* \sqrt{S_{id}} \sqrt{S_{si}} \sqrt{E_b} n_3}{\sigma_N^2 (\alpha_i^2 |h_{id}|^2 S_{id} + 1)} \right\}, \quad (4.8)$$

where N is the number of relays participating in communication. The total SNR, χ_{total} , at the destination is given as

$$\chi_{total} = \chi_{sd} + \sum_{i=1}^N \frac{\chi_{si} \chi_{id}}{\chi_{si} + \chi_{id}}, \quad (4.9)$$

where $\chi_{ij} = \frac{|h_{ij}|^2 S_{ij}}{\sigma_N^2}$. The received SNR is the addition of two different SNRs; one from the direct link between the source and destination while the other is the sum of individual SNRs of the relayed links.

4.2 System Outage Analysis

In this section, we show that the received SNR at the destination node, shown in (9), can be expressed as a lognormal RV with mean μ_{x_t} , and variance $\sigma_{x_t}^2$.

Having said that, the outage probability is given as

$$P \{ \chi_{total} \leq \tau \} = Q \left(\frac{\mu_{x_t} - \tau}{\sigma_{x_t}} \right), \quad (4.10)$$

where Q represents the Q-function; where $Q(x) = \int_x^\infty \frac{1}{\sqrt{2\pi}} \exp\left(-\frac{y^2}{2}\right) dy$ and τ is the modulation dependent threshold. We now proceed step by step to show that χ_{total} is a lognormal RV. Consider the following lemma:

Let $Z = XW$, where X is a lognormal RV with mean μ_x and variance $\sigma_{x(dB)}^2$ and W is a unit mean exponential RV, then Z is also lognormal with mean $\mu_z = \frac{C}{\zeta} + \mu_{x(dB)}$ and variance $\sigma_z^2 = \frac{1}{\zeta^2} \left(\frac{\pi^2}{6} + \zeta^2 \sigma_x^2 \right)$, where $C = 0.5772$ and $\zeta = \frac{\ln(10)}{10}$.

Proof. The products involving a lognormal RV can be well approximated by another lognormal RV [25]. The composite distribution of squared envelope of an exponential-lognormal RV can be expressed as

$$P_z(z) = \int_0^\infty \frac{1}{x} e^{-\frac{z}{x}} \times \frac{1}{x\sigma_x\zeta\sqrt{2\pi}} \exp\left\{-\frac{(10\log_{10}\{x\} - \mu_{x(dB)})^2}{2\sigma_x^2}\right\} dx. \quad (4.11)$$

We start our procedure by finding the first moment, i.e.,

$$\mathbb{E}[10\log_{10}(Z)] = \int_0^\infty 10\log_{10}(z) \int_0^\infty \frac{1}{x} e^{-\frac{z}{x}} \times \frac{1}{x\sigma_x\zeta\sqrt{2\pi}} \exp\left\{-\frac{(10\log_{10}\{x\} - \mu_{x(dB)})^2}{2\sigma_x^2}\right\} dz dx. \quad (4.12)$$

By change of variables and solving the inner integral, the above expression can be written as

$$\mathbb{E}[10\log_{10}(Z)] = \frac{1}{\sigma_x\zeta\sqrt{2\pi}} \int_{-\infty}^\infty \exp\left\{-\frac{(y - \mu_{x(dB)})^2}{2\sigma_x^2}\right\} dy. \quad (4.13)$$

Solving this equation gives us the first moment of the related normal RV, i.e.,

$$\begin{aligned} \mu_z &= \mathbb{E}[10\log_{10}(Z)] \\ &= -\frac{C}{\zeta} + \mu_{x(dB)}, \end{aligned} \quad (4.14)$$

where $C \simeq 0.5772$ is the Euler's constant. Similarly the second order moment can be found by same procedure and expressed as

$$\mathbb{E} \left[(10 \log_{10}(Z))^2 \right] = \frac{1}{\zeta^2} \left\{ C^2 + \frac{\pi^2}{6} - 2\zeta \mu_{x(dB)} C + \zeta^2 (\mu_{x(dB)}^2 + \sigma_{x(dB)}^2) \right\}. \quad (4.15)$$

The variance of Z can be calculated from (4.14) and (4.15), i.e.,

$$\begin{aligned} \sigma_Z^2 &= \mathbb{E} \left[10 \log_{10}(Z)^2 \right] - \mathbb{E} \left[10 \log_{10}(Z) \right]^2 \\ &= \frac{1}{\zeta^2} \left(\frac{\pi^2}{6} + \zeta^2 \sigma_x^2 \right), \end{aligned} \quad (4.16)$$

□

where $\zeta = \frac{\ln(10)}{10}$. Lemma 1 provides a proof that the power received through direct path is lognormal distributed. We now focus on the relayed paths. Consider the following propositions for the numerator and denominator of the second term in (4.9).

Proposition 1.

If $X_i \sim \text{lognormal}(\mu_i, \sigma_i^2)$ are n independent and identically distributed (i.i.d) lognormal RVs, and $Y = \prod_{i=1}^n X_i$, then Y will also be a lognormally distributed such that

$$Y(\sum_{i=1}^n \mu_i, \sum_{i=1}^n \sigma_i^2). \quad (4.17)$$

Proof. For proof, see [25] □

Proposition 2.

Let $X_i \sim \text{lognormal}(\mu_i, \sigma_i^2)$ be i.i.d lognormal RVs then, $Y = \sum_{i=1}^n X_i$ is another lognormal RV with

$$\sigma_Y^2 = \ln \left[\frac{\sum_{i=1}^n (e^{2\mu_i + \sigma_i^2}) (e^{\sigma_i^2} - 1)}{\sum_{i=1}^n (e^{\mu_i + \sigma_i^2/2})^2} + 1 \right], \quad (4.18)$$

$$\mu_Y = \ln \left[\sum_{i=1}^n (e^{\mu_i + \sigma_i^2/2}) \right] - \frac{\sigma_Y^2}{2}. \quad (4.19)$$

Proof. For proof, see Fenton-Wilkinson [26] □

Corollary 1.

If each lognormal RV X_i has identical variance parameter, i.e., $\sigma_i^2 = \sigma^2 \forall i$, then the mean and variance of lognormal RV $Y = \sum_{i=1}^n X_i$ can be expressed as

$$\sigma_Y^2 = \ln \left[(e^{\sigma^2} - 1) \frac{\sum_{i=1}^n e^{2\mu_i}}{\sum_{i=1}^n (e^{\mu_i})^2} + 1 \right], \quad (4.20)$$

$$\mu_Y = \ln \left[\sum_{i=1}^n (e^{\mu_i}) \right] - \frac{\sigma_Y^2}{2} + \frac{\sigma^2}{2}. \quad (4.21)$$

Proposition 1 and 2 will be used to approximate the product and sum of lognormal RVs in the second term of (4.9). For the ratio, consider the following lemma.

Lemma 1.

Let $Z = \frac{X}{Y}$, where X and Y are two lognormal RVs with mean μ_X, μ_Y and variances σ_X^2, σ_Y^2 , respectively, then Z is another lognormal RV with mean $\mu_Z = \mu_X - \mu_Y$ and variance $\sigma_Z^2 = \sigma_X^2 + \sigma_Y^2 - \sigma_{XY}$, where σ_{XY} is the covariance between X and Y .

Proof. Consider the logarithm of the ratio of two lognormal RVs, i.e., $\log(\frac{X}{Y}) = \log X - \log Y$, where X and Y are lognormal RVs. This implies that $\log X$

and $\log Y$ are normal RVs. Let's assume $\log X$ and $\log Y$ have means μ_x and μ_y , variances σ_x^2 and σ_y^2 , respectively. Covariance can be represented as σ_{xY} , which will be 0 if X and Y are independent. The difference R is then normally distributed having mean $\mu_R = \mu_x - \mu_y$ and variance $\sigma_R^2 = \sigma_x^2 + \sigma_y^2 - \sigma_{xY}$. The σ_{xy} can be expressed as

$$\sigma_{xY} = E[X^2]\mu_y + E[Y^2]\mu_x - \mu_x\mu_y, \quad (4.22)$$

To achieve $\frac{X}{Y}$, we know $\frac{X}{Y} = \exp\{R\}$, which shows that $\frac{X}{Y}$ itself is lognormally distributed with parameters μ_R and σ_R^2 . The relationship between the means and variances of a lognormal and its corresponding RV can be expressed as

$$\mathbb{E}\left[\frac{X}{Y}\right] = \mathbb{E}\left(e^R\right) = \exp\left\{\mu_R + \frac{1}{2}\sigma_R^2\right\} \quad (4.23)$$

$$\begin{aligned} \text{Var}\left[\frac{X}{Y}\right] &= \text{Var}\left(e^R\right) \\ &= \exp\left\{2\mu_R + 2\sigma_R^2\right\} + \exp\left\{2\mu_R + \sigma_R^2\right\} \end{aligned} \quad (4.24)$$

□

Theorem 4.1. *The total received SNR $\chi_{total} = \chi_{sd} + \sum_{i=1}^N \frac{\chi_{si}\chi_{id}}{\chi_{si} + \chi_{id}}$ can be approximated as a lognormal RV.*

Proof. From Lemma 1, each χ_{ij} is a lognormal RV where i, j denotes the transmitter and receiver nodes, respectively. From Lemma 2, Proposition 1 and Proposition 2, it can be proved that the ratio of lognormal RVs can be generalized with another lognormal RV. Hence each of the $N + 1$ terms in (4.9) have shown to be lognormal. In the final summation of lognormal RVs there may exist variables having different means and variances. From Proposition 2 again χ_{total} follows a lognormal distribution.

□

Chapter 5

Results and Analysis

In this chapter, we analyze the numerical results generated through simulations. Firstly, we will discuss the results regarding the performance of RFA scheme. This scheme has been analyzed under different possible scenarios, where parameters like path loss exponent, number of relays, cell diameter has been varied. Overall system's outage probability has been taken as the prime QoS parameter for the analysis. After RFA, the effect of different channel impairments, like shadowing, multipath fading, and path loss exponent, in a HetNet has been analyzed. Cooperation and relay selection method has also been proposed in the particular section. Again different parameters like path loss, shadowing coefficient, threshold SNR has been varied and analyzed for a complete analysis. Average system's coverage probability has been taken the QoS parameter for this particular analysis. Extensive simulations were performed in order to validate the numerical results.

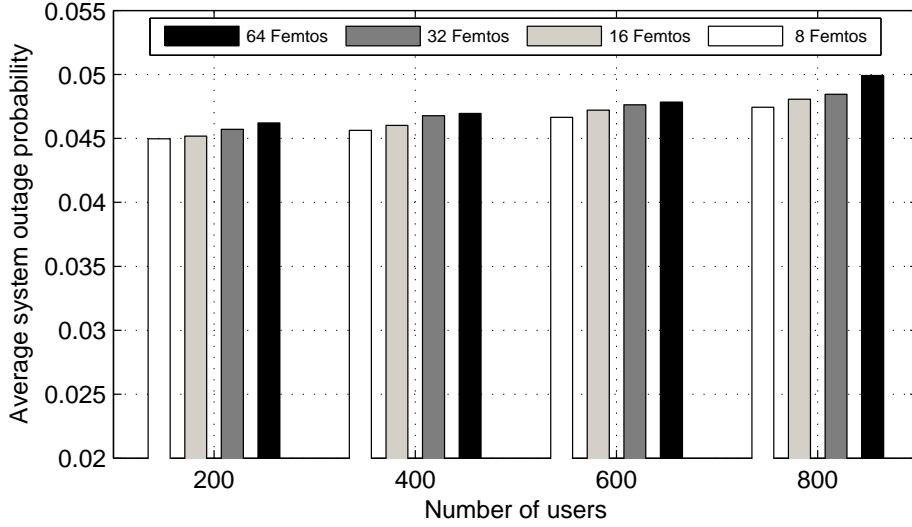


Figure 5.1: Effects of β on coverage for various number of participating relays.

5.1 Reverse Frequency Allocation

In our simulation environment, we randomly distribute circular-shaped femtocells within a hexagonal macrocell. Open access mode is simulated in our simulations for the femtocells. Macrocell base station (MBS) and femto access points (FAPs) are assumed to have omnidirectional antennas. Transmission power of MBS and FAP is fixed to be 20 and 0.2 Watts, respectively, while the transmit power of both MUE and FUE is fixed to 0.2 Watts. The users are uniformly placed in the macrocell, where at least one user is placed in each femtocell. Parameters used for the simulations are shown in Table 1. User outage for 2-region and 4-region RFA is analyzed.

Fig. 5.1 and 5.2, shows the outage probability in a 2-region RFA scheme with the 4-region RFA. These graphs analyze the overall system outage for a macrocell having a radius of 1 Km with varying number of users and with varying total number of femtocells. The path loss exponent, β , is taken to be

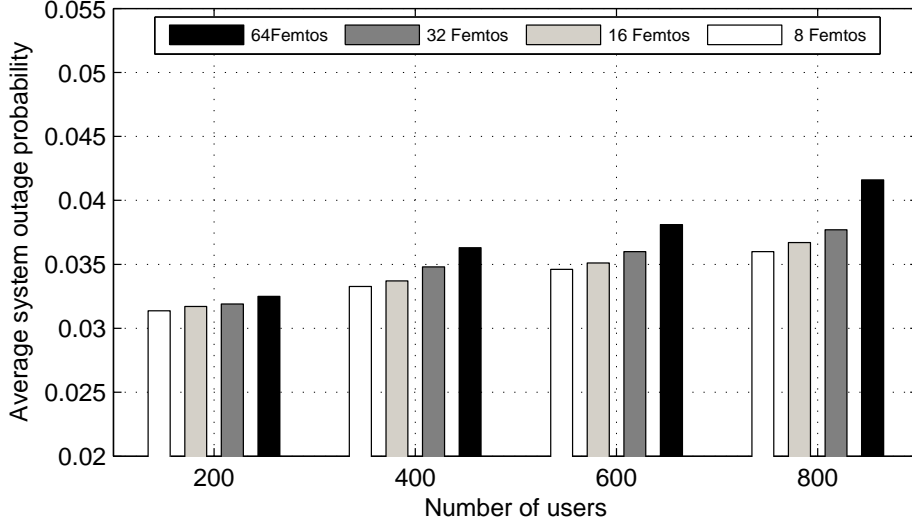


Figure 5.2: Effects of β on coverage for various number of participating relays.

2 in this case. It can be observed that as the number of users increases, the average system outage probability also increases. This increase in the system outage is due to the cross-tier interference, i.e., interference from MUEs to FUE in the uplink direction. Also with the increasing number of femtocells, the co-tier interference also increases, i.e., interference from FAPs to FUEs in the downlink direction. Therefore, in both cases, i.e., either increasing number of users and/or femtocells, the system outage probability increases. In Fig. 5.1, 2-region RFA scheme is analyzed. It divides the complete cell in 2 regions. Simulations were performed on different number of femtocells. For example, when 8 femtos are considered then each region contains 4 femtocells. Similarly, for 64 femtos, every region has 32 femtocells each and so on. From Figs. 5.1 and 5.2, we can see that 4-region RFA scheme outperforms 2-region RFA in terms of system outage probability. This reduction in system outage is due to the fact that 4-region RFA divides the complete single cell in such

a way that each region has less number of interferers.

Fig. 5.3 analyzes different RFA schemes i.e., 2-region, 4-region, and 8-region RFA, at different cell radii and different path loss exponents. 800 users and 64 femtocells were randomly distributed in the cell. In 8-region RFA, total area is divided among 8 regions. Frequency spectrum is divided in such a way that any region, at maximum, can have no more than 2 interfering regions. For example, R_3 will have R_1 and R_5 as its interfering regions. Similarly, R_4 has R_2 and R_6 as its interfering regions. On the other hand R_1 , R_2 , R_7 , and R_8 will have only one interfering region. As the cell radius increases, the distance between the FUE (victim) and the MUE and interfering FAPs (aggressor) also increases, alleviating the SINR of FUE. This improvement in performance is not as significant in 8-region RFA as it is in 4-region RFA scheme. This is due to the fact that as the number of regions increases for a fixed cell radius, not only the interfering regions come close but also the size of each region decreases, yielding higher co-tier and cross-tier interferences. Hence at smaller cell radii 8-region RFA performs almost equal to the 4-region RFA scheme.

On the other hand, it can also be seen that as the cell radius increases, the difference between the performance of 2-region and 4-region RFA also increases. For larger cell radii, the 4-region RFA significantly improves the performance in terms of outage probability. For example, at the cell radius of 4 Km with 800 users and $\beta = 2$, the 2-region RFA scheme provides an average system outage probability approximately equal to 5%, but in the 4-region RFA with same parameters, the average system outage probability decreases to 2%. Hence large number of users will be in coverage. Similarly,

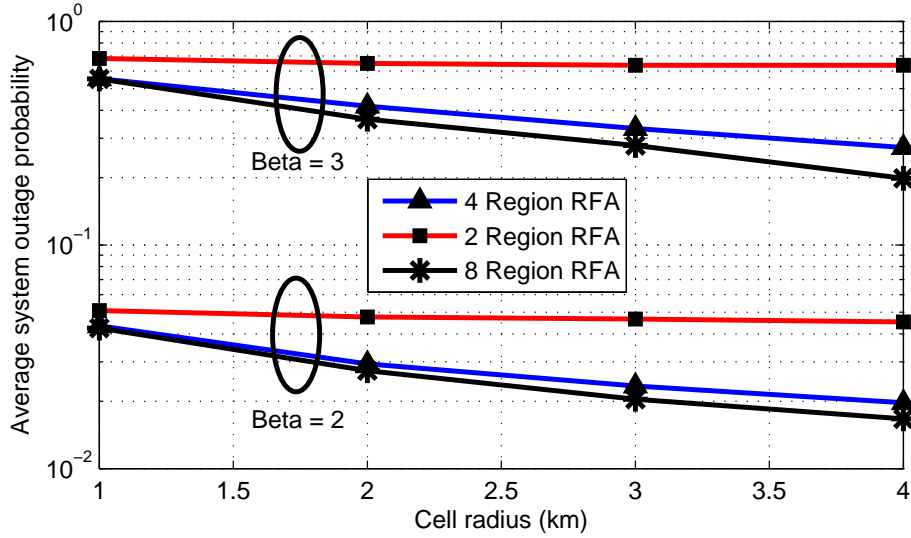


Figure 5.3: Effects of β on coverage for various number of participating relays.

for the larger path loss exponents, β , it can be seen that the 4-region RFA outperforms the 2-region RFA. For example, the difference in system outage probability for two schemes at a radius of 4Km with $\beta = 2$ is 3%. While at $\beta = 3$, this difference is increased up to approximately 40%. So, we can say that for larger cell radius or larger path loss exponent, the 4-region RFA completely outperforms the 2-region RFA.

Fig. 5.4 shows the contour plot that provides the average system outage probability that will be faced in any cell with a particular radius and varying number of femtocells for a 4-region RFA. These simulations were done with 600 users and β is taken to be 3. It can be observed that at a radius of 2 Km, the outage probability for 80 femtocells is around 46%. If this outage probability needs to be reduced for same number of cell users to 40%, then the maximum number of allowed femtocells should not be greater than 30. Hence an upper bound on the number of femtocells can be evaluated for

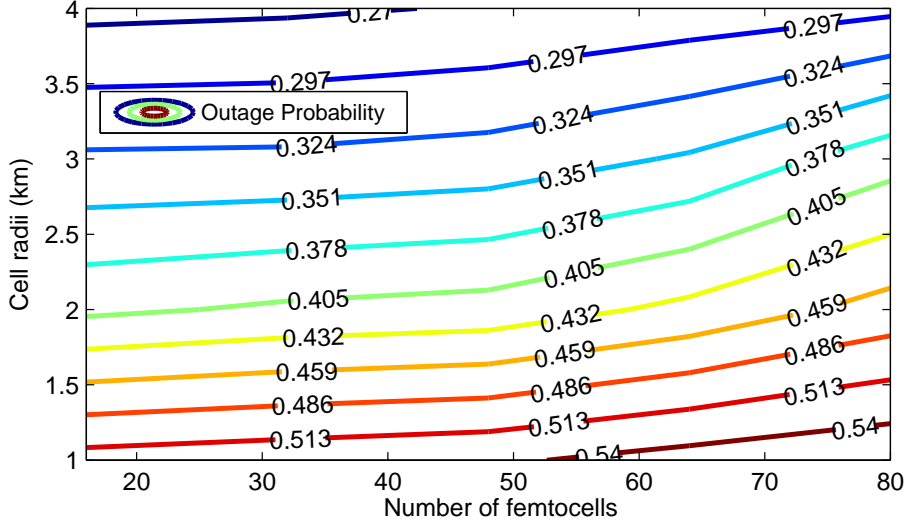


Figure 5.4: Effects of β on coverage for various number of participating relays.

varying cell radii.

5.2 Cooperative Networks with individual channel impairments

In this section, we verify the derived analytical expressions through computer simulations and provide the effects of various parameters on the performance of the system. We first verify the lognormal approximations that we performed in Lemma 1, Lemma 2, and Theorem 1, respectively. For the ease of notation, we refer to approximation of exponential-lognormal (Lemma 1) to χ_{ij} which is another lognormal. Fig. 5.5(a) compares the analytical and simulated results of cumulative distribution function (CDF) of RV χ_{ij} . The simulation curve is obtained by generating independent lognormal and exponential RVs and multiplying them. 10^7 iterations were performed to obtain

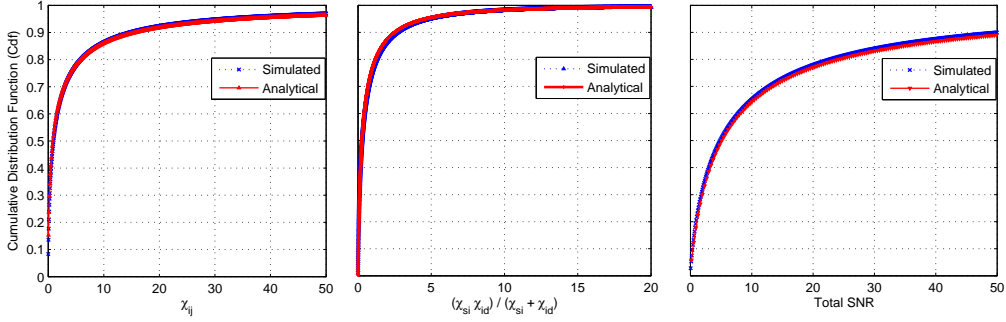


Figure 5.5: The CDF of (a) χ_{ij} , product of exponential & lognormal RV., (b) SNR from relayed path., (c) Total SNR of the system.

the CDF of the resultant RV. The analytical result is obtained by simply generating a lognormal RV with mean and variance as obtained in Lemma 1. Both the curves match closely and the mean squared error between them was found to be of the order of 10^{-6} .

Fig. 5.5(b) represents the analytical result proved in Lemma 2. It shows the CDF of a lognormal RV, which is an approximated result of the ratio of lognormal RVs. This ratio is itself a product of two lognormal RVs in its numerator and sum of lognormals in the denominator. The results follow almost identical CDF curves. Fig. 5.5(c) shows the CDF of total SNR proved in Theorem 1. The cumulative SNR expressed in (4.9) can be considered as a summation of individual lognormals as proved from Fig. 5.5(a) and Fig. 5.5(b). These lognormals can also have different means and variances. The resulting parameters can be calculated from (4.18) and (4.19) and are plotted in the figure. In all of the above cases, the standard deviation of shadowing for each RV is identical and taken to be 8dB.

Fig. 5.6 shows the effects of increasing the number of relays on the cov-

erage probability with respect to different path loss exponents, β . For each i, j link in Fig. 2, the d_{ij} is kept at 150 m, while the $\sigma_{ij} = \sigma = 8$ dB and threshold $\tau = -20$ dB. It can be observed from the figure that there is an increase in the coverage probability as the number of relays is increased. It can be further observed that as the number of relays increases from 0 to 2, there is a significant change in the coverage probability, however, this change becomes very small for larger number of relays. A diminishing trend in the diversity gain is seen as the number of relay increases.

The SNR threshold versus coverage probability trend is analyzed for different number of relays in Fig. 5.7. For $\beta = 2$ and $\sigma = 8$ dB, it can be observed that the coverage probability is decreased with an increase in the threshold. However, the coverage of the non-cooperative case is least amongst all cases and it increases as the number of relays is increased due to the increased diversity gain that additional relays offer. However, at higher values of threshold, the coverage becomes same for all cases because more and more nodes will start to be in outage until comes a point where every receiver node in the system will have received signal's strength below the SNR threshold.

The difference in system's coverage probability in both large and small cells while considering different standard deviation of shadowing is shown in Fig. 5.8. Same values of shadowing has been assumed for all the links present in each particular scenario. For large cells, distance between the source and end user can be up to 1000 meters, while a relay can be selected if it is present within 100 meters from the destination. In case of a small cell, $d_{sd} = 400$ meters, while relays can be selected within 40 meters of radius. Three operational relays are considered with $\beta = 2$. It can be seen

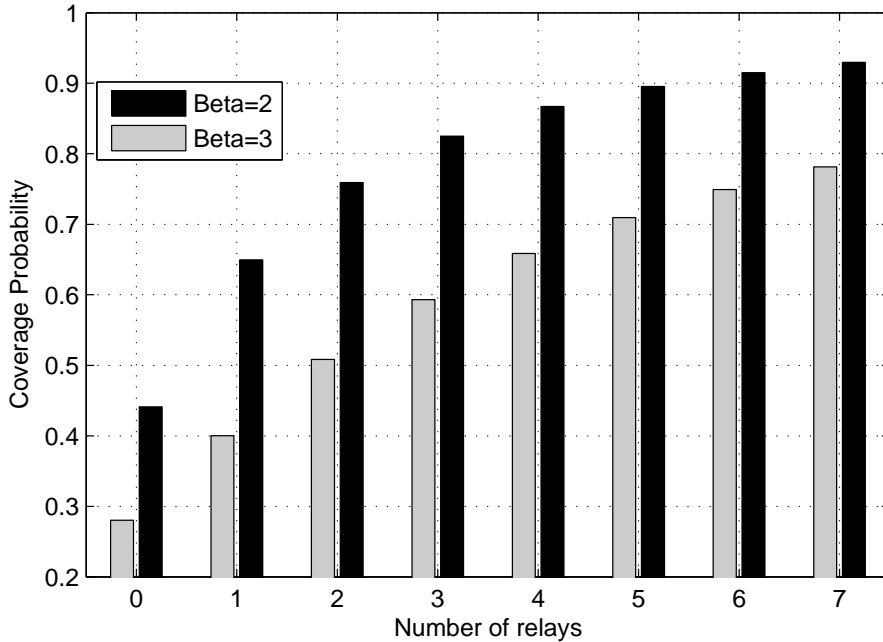


Figure 5.6: Effects of β on coverage for various number of participating relays.

for both cases that at lower values of standard deviation, the coverage probability is higher. This is because the severity of shadowing is small and a coverage gain of almost 14% is seen at a threshold of -20 dB for large cells. However, as the threshold is increased after -2 dB, the $\sigma = 12$ dB curve outperforms. This is because the shadowing models the fluctuations in received power. These fluctuations become large for larger σ . Therefore, even at higher thresholds, one can still get a favorable shadowing outcome, which eventually increases the coverage probability of the network. Hence in designing systems where shadowing becomes considerable channel impairment, a sufficient shadow margin is necessary to compensate for the losses. Overall the coverage of small cells outperforms the large cell environment because of the small distances between communication entities.

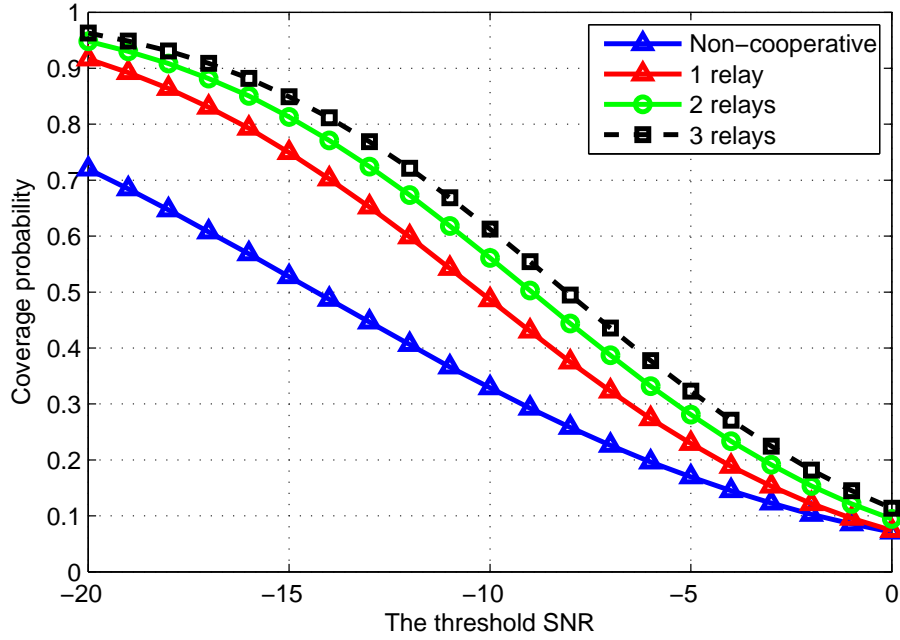


Figure 5.7: Effects of threshold SNR on system's coverage.

Table 5.1: Simulation Parameters

Parameter	Value
Power of MBS	20 Watts
Power of MUE	0.2 Watts
Power of FAP	0.2 Watts
Power of FUE	0.2 Watts
Femto Radius	50 meters
Macrocell radius	1 to 4 Km
P _{th}	-50dB

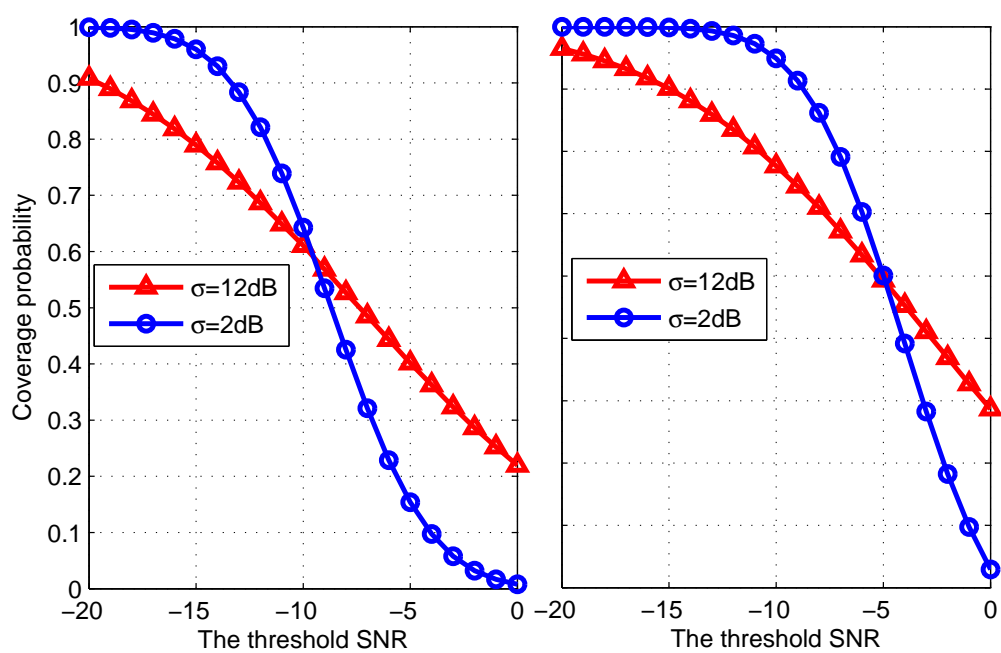


Figure 5.8: Variation in system's coverage for values of σ in large (left) and small (right) cell environments

Chapter 6

Conclusions and Future Work

6.1 Conclusions

Dense deployment of femtocells provides high data rates to the indoor users. It also enables the network operators to offload the traffic from macro base station. In order to achieve a good QoS and coverage, co-tier and cross-tier interferences are the major problems among the femto-femto and femto-macro networks, respectively. There have been multiple techniques that were proposed and analyzed by different authors around the world in order to tackle above mentioned interferences. There is always a trade-off between spectral efficiency and no. of users served. The reverse frequency allocation scheme is one of the robust techniques in term of interference mitigation and spectral efficiency, particularly in downlink traffic. We have proposed an RFA scheme in the downlink by dividing the cell into multiple regions. Specifically, we studied the 2, 4, and 8-region RFA schemes. Special feature of this RFA scheme is that despite of dividing the band into different sub-bands, still complete band is utilized with a single cell. Hence, improving

the spectral efficiency to its maximum level. Another feature of RFA scheme is that it eliminates the BTS, which has infinite power, as an interfering entity within a cell. The possible interferers are the MUEs or the FAPs which are highly constrained in terms of transmitting power. That reduces the overall interference in the system. Simulation results show that the 4-region RFA with optimal cell radii provides a reduced average system outage probability as compared to the 2-region RFA in terms of a certain number of users and femtocells. Moreover, by increasing the cell radius, 4-region RFA outperforms the 2-region RFA in term of system outage for certain values of path loss exponent.

Enabling D2D cooperation in a heterogeneous network provides better coverage and high data rates. Cooperation involves mobile devices relaying the data for some other end user increasing the overall system's throughput. As relaying is done in large area networks consisting of different types of terrains. Shadowing must be considered along with channel fading and path loss for efficient modeling of large-scale networks. In this thesis, we have modeled the effects of these three parameters on the coverage of a cooperative HetNet performing D2D, where idle FUEs cooperate with a MUE. We also proved that ignoring shadowing or just incorporating the above mentioned channel impairments as a single entity will result in impractical analysis. Including the exponential fading and lognormal shadowing yield a PDF for which no closed form PDF exists in the literature. We found a closed form expression for the resulting mean and variance using same PDF. It has been shown through analysis that the SNR of both individual link and the relayed links can be modeled by a lognormal RV, also the resulting PDF of the

combined signals at the destination can also be modeled through simple lognormal distribution. Representation of resulting PDFs through lognormal distribution results in ease of analysis to a greater level despite of maintaining high efficiency.

6.2 Future Work

The analysis of RFA scheme with higher multiple regions, its spectral efficiency, and complexity analysis is left as a future work. Also the effect of multiple cells in terms of cross-tier interference can also be observed. Although that interference will definitely be negligible due to very low transmitting power interferers and large distances. For the second portion of the thesis, the bit error rate analysis could also be another QoS parameter that can be analyzed in the developed scenario/infrastructure. Interference including all three channel impairments, i.e., shadowing, path loss, and fading from neighboring macrocells in a multi-cell environment is left as a future work. Different optical combining techniques other than MRC, like minimum mean square error (MMSE) can also be implemented in the presence of interference for more optimized results.

Bibliography

- [1] Informa Telecoms & Media, “Femtocell Market Status,” Femtoforum whitepaper, 2011.
- [2] Presentations by ABI Research, Picochip, Airvana, IP access, Gartner, Telefonica Espana, “Home Access Points and Femtocells;,” *2nd Intl. Conf.*. Available: http://www.avrenevents.com/dallasfemto2007/purchase_presentations.html
- [3] V. Chandrasekhar and J. G. Andrews, “Uplink capacity and interference avoidance for two-tier femtocell networks,” *IEEE Trans. Wireless Commun.*, vol. 8, pp. 3498-3509, Jul. 2009.
- [4] M. Z. Chowdhury, Y. M. Jang, Z. J. Haas, “Cost-effective frequency planning for capacity enhancement of femtocellular networks,” *Wireless Personal Commun.*, vol. 60, Issue 1, pp. 83-104, Sept. 2011.
- [5] Y. Li, C. Song, D. Jin, S. Chen, “A dynamic graph optimization framework for multihop device-to-device communication underlying cellular networks,” *IEEE Wireless commun.*, vol. 21, no. 5, pp. 52-61, 2014.

- [6] O. Yilmaz, Z. Li, K. Valkealahti, M. A. Uusitalo, M. Moisio, P. Lunden, C. Wijting, “Smart mobility management for D2D communications in 5G networks,” *IEEE Wireless commun. and networking conference (WCNC)*, March 2014.
- [7] J. Zhang, de la Roche, E. Liu, “Introduction, in femtocells: technologies and deployment”, John Wiley Sons, Ltd, Chichester, UK, 2009.
- [8] V. Chandrasekhar, J. G. Andrews and A. Gatherer, “Femtocell networks: a survey”, *IEEE Commun. Mag.*, vol. 46, no. 9, pp. 59-67, Sept. 2008.
- [9] S.P. Yeh, S. Talwar, S.-C. Lee, and H. Kim, “WiMAX femtocells: A perspective on network architecture, capacity, and coverage,” *IEEE Commun. Mag.*, vol. 46, no. 10, pp. 58-65, Oct. 2008.
- [10] D. Lupez-Ptrez, A. Valcarce, G. de la Roche, and J. Zhang, “OFDMA femtocells: A roadmap on interference avoidance,” *IEEE Commun. Mag.*, vol. 47, no. 9, pp. 41-48, Sept. 2009.
- [11] T. Zahir, K. Arshad, A. Nakata, K. Moessner, “Interference management in femtocells,” *IEEE Commun. Surveys & Tutorials*, vol. 15, no. 1, pp. 293-311, First Quarter 2013.
- [12] K. Cho, W. Lee, D. Yoon, K. Hyun; Yun-Sung Choi, “Resource alloation for orthogonal and co-channel femtocells in a hierarchical cell structure,” *IEEE 13th Int. Symposium on Consumer Electron. (ISCE)*, pp. 655-656, May 2009.
- [13] P. Lee, T. Lee, J. Jeong, J. Shin, “Interference management in LTE femtocell systems using fractional frequency reuse,” *12th Int. Conf. on Adv.*

- Commun. Tech.: ICT for Green Growth and Sustainable Development (ICTACT)*, vol. 2, pp. 1047-1051, Feb. 2010.
- [14] N. Saquib, E. Hossain, D. I. Kim, "Fractional frequency reuse for interference management in LTE-advanced hetnets," *IEEE Commun. Surveys & Tutorials*, vol. 20, no. 2, pp. 113-122, April 2013.
- [15] T. Zahir, K. Arshad, Y. Ko, and K. Moessner, "A downlink power control scheme for interference avoidance in femtocells," *7th Int. Wireless Commun. and Mobile Computing Conf. (IWCMC)*, pp. 1222-1226, July 2011.
- [16] M. Z. Chowdhury, Y. M. Jang, Z. J. Haas, "Interference mitigation using dynamic frequency reuse for dense femtocell network architectures," *2nd Int. Conference on Ubiquitous and Future Net. (ICUFN)*, pp. 256-261, June 2010.
- [17] P. Jacob, A. James, A. S. Madhukumar, "Downlink interference Reduction through Reverse Frequency Allocation," *Int. Conf. on Commun. Systems (ICCS)*, pp. 329-333, Nov. 2012.
- [18] M. Patzold, "Mobile Fading Channels," John Wiley and Sons, Ltd, U.K., 2002.
- [19] M. Nakagami, "The m Distribution. A General Formula for Intensity Distribution of Rapid Fading," in W.C. Hoffman (ed.), *Statistical Methods in Radio Wave Propagation*, New York, 1960.
- [20] S.S. Ikki, M. Feteiha, M. Uysal, "Performance analysis of cooperative diversity networks with imperfect channel estimation over Rician fading

- channels,” IEEE 17th International Conference on Telecommunications (ICT), pp. 160-165, April 2010.
- [21] J. Adeane, M. Rodrigues, I. J. Wassell, ” Characterisation of the performance of cooperative networks in Ricean fading channels,” IEEE 12th International Conference on Telecommunications (ICT), pp. 3-6, 2005.
- [22] A. M. Zaid, B. Hamdaoui, C. Xiuzhen, T. Znati, M. Guizani, “Improving macrocell downlink throughput in Rayleigh fading channel environment through femtocell user cooperation,” *IEEE Trans. Wireless Commun.*, vol.12, pp. 6488-6499, Dec. 2013.
- [23] T. M. Cover and A. A. El Gamal, “Capacity theorems for the relay channel,” *IEEE Trans. Inform. Theory*, vol. 25, no. 5, pp. 572-584, Sept. 1979.
- [24] G. L. Stuber, “Principles of Mobile Communication,” 2nd Ed. Springer International, 2011.
- [25] N. B. Mehta, J. Wu , A. F. Molisch, and J. Zhang, “Approximating a sum of random variables with a lognormal,” *IEEE Trans. Wireless Commun.*, vol. 6, no. 7, pp. 2690-2699, July 2007.
- [26] L. F. Fenton, “The sum of lognormal probability distributions in scatter transmission systems,” *IEEE IRE Trans. Commun. Systems*, vol. 8, no. 1, pp. 57-67, 1960.